1 EFMs of the example

We consider the network $\mathcal{N} = (\mathfrak{M}, \mathfrak{R}, S, \mathrm{Irr})$ in Fig. 1 of the main text with the stoichiometric matrix

$$S = \begin{pmatrix} 1 & -1 & 0 & 0 & 0 & 0 & 0 & 0 & 0 & 0 & 0 & 0 \\ 0 & 1 & -1 & 0 & -1 & 0 & 0 & 0 & 0 & 0 & 0 & 0 \\ 0 & 1 & 0 & -1 & 0 & -1 & 0 & 0 & 0 & 0 & 0 & 0 \\ 0 & 0 & 0 & 0 & 1 & 0 & 0 & 1 & -1 & 0 & -1 & 0 \\ 0 & 0 & 0 & 0 & 0 & 1 & -1 & -1 & 0 & 0 & 0 & 0 \\ 0 & 0 & 0 & 0 & 0 & 0 & 0 & 0 & 0 & 0 & 1 & -1 \\ 0 & 0 & 0 & 0 & 0 & 0 & 0 & 0 & 1 & -1 & 0 & 0 \end{pmatrix}.$$

There exist 18 EFMs with the following supports: $\{1, 2, 3, 4\}$, $\{1, 2, 3, 5, 6, 8\}$, $\{1, 2, 3, 6, 7\}$, $\{1, 2, 3, 6, 8, 9, 10\}$, $\{1, 2, 3, 6, 8, 11, 12\}$, $\{1, 2, 4, 5, 9, 10\}$, $\{1, 2, 4, 5, 11, 12\}$, $\{1, 2, 5, 6, 7, 9, 10\}$, $\{1, 2, 5, 6, 7, 11, 12\}$, $\{1, 2, 5, 6, 8, 9, 10\}$, $\{1, 2, 5, 6, 8, 11, 12\}$, $\{3, 4, 5, 6, 8\}$, $\{3, 5, 9, 10\}$, $\{3, 5, 11, 12\}$, $\{4, 6, 7\}$, $\{4, 6, 8, 9, 10\}$, $\{4, 6, 8, 11, 12\}$, $\{9, 10, 11, 12\}$. The sets $\{3, 5, 9, 10\}$, $\{3, 5, 11, 12\}$, $\{9, 10, 11, 12\}$ correspond to reversible EFMs, which can carry flux in both directions.

The oriented circuits of the oriented matroid $\mathcal{M}_S$ include these EFMs and the 6 signed sets $\{-7, +8, +9, +10\}$, $\{+1, +2, +4, +5, +7, -8\}$, $\{-3, +5, +7, -8\}$, $\{+1, +2, +5, +6, +7, -8\}$, $\{+1, +2, +4, +5, -6, -8\}$, $\{-7, +8, +11, +12\}$, which do not correspond to a feasible flux vector. In each of these, there is an irreversible reaction with negative flux.

2 Oriented matroids

Let U be a set and $\mathcal{C}$ a family of signed subsets of U. The pair $\mathcal{M} = (U, \mathcal{C})$ is called an *oriented matroid* if the following *circuit axioms* are satisfied (Björner *et al.*, 1999):

1. $\emptyset \notin \mathcal{C}$.
2. If $X \in \mathcal{C}$, then $-X \in \mathcal{C}$.
3. For all $X, Y \in \mathcal{C}$, if $\mathrm{supp}(X) \subseteq \mathrm{supp}(Y)$, then $X = Y$ or $X = -Y$.
4. For all $X, Y \in \mathcal{C}$, $X \neq -Y$ and $u \in X^+ \cap Y^-$ there is a $Z \in \mathcal{C}$ with $Z^+ \subseteq (X^+ \cup Y^+) \setminus \{u\}$ and $Z^- \subseteq (X^- \cup Y^-) \setminus \{u\}$.

3 Contraction via deletion in the dual matroid

Let $\mathcal{M} = (U, \mathcal{C})$ be an oriented matroid and let $A \subseteq U$. The family $\mathcal{C} \setminus A = \{X \in \mathcal{C} \mid \mathrm{supp}(X) \subseteq U \setminus A\}$ is the set of circuits of an oriented matroid $\mathcal{M} \setminus A = (U \setminus A,\ \mathcal{C} \setminus A)$, which is called the *deletion of A from* $\mathcal{M}$ (Björner *et al.*, 1999, p. 110). An alternative notation for the contraction $\mathrm{contr}_H(\mathcal{M})$ of $\mathcal{M} = (U, \mathcal{C})$ on $H \subseteq U$ is to write $\mathcal{M}/A$ with $A = U \setminus H$ (Björner *et al.*, 1999, p. 111).

Proposition 3.4.9 in (Björner *et al.*, 1999, p. 123) states that for an oriented matroid $\mathcal{M} = (U, \mathcal{C})$ and $A \subseteq U$ we have

$$\begin{aligned} (\mathcal{M} \setminus A)^* &= \mathcal{M}^*/A \\ (\mathcal{M}/A)^* &= \mathcal{M}^* \setminus A, \end{aligned}$$

where $\mathcal{M}^*$ is the dual oriented matroid of $\mathcal{M}$. Since $\mathcal{M}^{**} = \mathcal{M}$, the contraction of $\mathcal{M}$ on $H = U \setminus A$ can be realized by the deletion of A in the dual matroid $\mathcal{M}^*$.

If an oriented matroid $\mathcal{M}_B = (U, \mathcal{C})$ is represented by a matrix $B \in \mathbb{R}^{m \times |U|}$, then the dual matroid $\mathcal{M}_B^*$ can be obtained in the following way (Ziegler, 1995, p.166). Suppose the matrix B representing $\mathcal{M}_B$ is given as $B = (E_r \mid Q)$, where E_r is the identity matrix of r elements. Then the dual matroid $\mathcal{M}_B^*$ is represented by the matrix $C = (-Q^\intercal \mid E_{n-r})$. Thus to compute the dual of the oriented matroid $\mathcal{M}_B$ we have to bring B to the form $B = (E_r \mid Q)$, which can be done by Gaussian elimination. To perform the contraction of $\mathcal{M}_B$ on $H = U \setminus A$, we delete A in $\mathcal{M}_B^*$. This is done by removing in the matrix $C \in \mathbb{R}^{|U| \times m}$ that represents $\mathcal{M}_B^*$ the columns corresponding to $A \subset U$. Finally, we compute $(\mathcal{M}_B^* \setminus A)^* = (\mathcal{M}_B/A)$. Note that with this approach no combinatorial explosion will occur like in Fourier-Motzkin elimination.

Example 1. The oriented matroid $\mathcal{M}_S = (\mathfrak{R}, \mathcal{C})$ we consider here is given by the set of reactions $\mathfrak{R} = \{1, \ldots, 12\}$ of the network in Fig. 1 of the main text and represented by its stoichiometric matrix $S \in \mathbb{R}^{|\mathfrak{M}| \times |\mathfrak{R}|}$, which can be found in Sect. 1 of the supplement.

To compute the dual matroid $\mathcal{M}_S^*$ we have to bring S to the form $(E_r \mid Q)$, which can be done by first bringing the matrix into the reduced row echelon form, e.g. using Gaussian elimination. The result is the following matrix:

$$S^{\mathrm{rref}} = \begin{array}{c} \begin{matrix} \boxed{1} & \boxed{2} & \boxed{3} & \boxed{4} & \boxed{5} & \boxed{6} & \boxed{7} & \boxed{8} & \boxed{9} & \boxed{10} & \boxed{11} & \boxed{12} \end{matrix} \\ \begin{pmatrix} 1 & 0 & 0 & -1 & 0 & 0 & -1 & -1 & 0 & 0 & 0 & 0 \\ 0 & 1 & 0 & -1 & 0 & 0 & -1 & -1 & 0 & 0 & 0 & 0 \\ 0 & 0 & 1 & -1 & 0 & 0 & -1 & -2 & 0 & 1 & 0 & 1 \\ 0 & 0 & 0 & 0 & 1 & 0 & 0 & 1 & 0 & -1 & 0 & -1 \\ 0 & 0 & 0 & 0 & 0 & 1 & -1 & -1 & 0 & 0 & 0 & 0 \\ 0 & 0 & 0 & 0 & 0 & 0 & 0 & 0 & 1 & -1 & 0 & 0 \\ 0 & 0 & 0 & 0 & 0 & 0 & 0 & 0 & 0 & 0 & 1 & -1 \end{pmatrix} \end{array}$$

Since we want to have an identity matrix in the front we have to change the order of the columns of S^{rref}:

$$B = \begin{array}{c} \begin{matrix} \boxed{1} & \boxed{2} & \boxed{3} & \boxed{5} & \boxed{6} & \boxed{9} & \boxed{11} & \boxed{4} & \boxed{7} & \boxed{8} & \boxed{10} & \boxed{12} \end{matrix} \\ \begin{pmatrix} 1 & 0 & 0 & 0 & 0 & 0 & 0 & -1 & -1 & -1 & 0 & 0 \\ 0 & 1 & 0 & 0 & 0 & 0 & 0 & -1 & -1 & -1 & 0 & 0 \\ 0 & 0 & 1 & 0 & 0 & 0 & 0 & -1 & -1 & -2 & 1 & 1 \\ 0 & 0 & 0 & 1 & 0 & 0 & 0 & 0 & 0 & 1 & -1 & -1 \\ 0 & 0 & 0 & 0 & 1 & 0 & 0 & 0 & -1 & -1 & 0 & 0 \\ 0 & 0 & 0 & 0 & 0 & 1 & 0 & 0 & 0 & 0 & -1 & 0 \\ 0 & 0 & 0 & 0 & 0 & 0 & 1 & 0 & 0 & 0 & 0 & -1 \end{pmatrix} \\ \begin{matrix} \underbrace{\hphantom{0\ 0\ 0\ 0\ 0\ 0\ 0\ 0\ 0}}_{E_r} & \underbrace{\hphantom{-1\ -1\ -1\ 0\ 0\ 0}}_{\mathbf{Q}} \end{matrix} \end{array}$$

The dual matroid $\mathcal{M}_S^*$ is represented by the matrix $C = (-Q^\intercal \mid E_{n-r})$, where $B = (E_r \mid Q)$. Thus

$$C = \begin{array}{c} \begin{matrix} \boxed{1} & \boxed{2} & \boxed{3} & \boxed{5} & \boxed{6} & \boxed{9} & \boxed{11} & \boxed{4} & \boxed{7} & \boxed{8} & \boxed{10} & \boxed{12} \end{matrix} \\ \begin{pmatrix} 1 & 1 & 1 & 0 & 0 & 0 & 0 & 1 & 0 & 0 & 0 & 0 \\ 1 & 1 & 1 & 0 & 1 & 0 & 0 & 0 & 1 & 0 & 0 & 0 \\ 1 & 1 & 2 & -1 & 1 & 0 & 0 & 0 & 0 & 1 & 0 & 0 \\ 0 & 0 & -1 & 1 & 0 & 1 & 0 & 0 & 0 & 0 & 1 & 0 \\ 0 & 0 & -1 & 1 & 0 & 0 & 1 & 0 & 0 & 0 & 0 & 1 \end{pmatrix} \\ \begin{matrix} \underbrace{\hphantom{0\ 0\ -1\ 1\ 0\ 0\ 1\ 0\ 0}}_{-Q^\intercal} & \underbrace{\hphantom{0\ 0\ 0\ 0\ 0\ 0}}_{E_{n-r}} \end{matrix} \end{array}$$

In order to contract $\mathcal{M}_S$ on $\mathrm{Irr} = \mathfrak{R} \setminus \mathrm{Rev}$ we delete $\mathrm{Rev} = \{3, 4, 5, 9, 10, 11, 12\}$ in $\mathcal{M}_S^*$, resp. the corresponding columns in C:

$$C' = \begin{array}{c} \begin{matrix} \boxed{1} & \boxed{2} & \boxed{6} & \boxed{7} & \boxed{8} \end{matrix} \\ \begin{pmatrix} 1 & 1 & 0 & 0 & 0 \\ 1 & 1 & 1 & 1 & 0 \\ 1 & 1 & 1 & 0 & 1 \\ 0 & 0 & 0 & 0 & 0 \\ 0 & 0 & 0 & 0 & 0 \end{pmatrix} \end{array}$$

The matrix C' represents the matroid $\mathcal{M}_S^* \setminus \mathrm{Rev}$. Since $(\mathcal{M}_S^* \setminus \mathrm{Rev})^* = (\mathcal{M}_S/\mathrm{Rev})$, we have to compute the dual of $\mathcal{M}_S^* \setminus \mathrm{Rev}$ in the same way as we did for $\mathcal{M}_S$. We first compute the reduced row echelon form:

$$(C')^{\mathrm{rref}} = \begin{array}{c} \begin{array}{ccccc} \boxed{1} & \boxed{2} & \boxed{6} & \boxed{7} & \boxed{8} \end{array} \\ \begin{pmatrix} 1 & 1 & 0 & 0 & 0 \\ 0 & 0 & 1 & 0 & 1 \\ 0 & 0 & 0 & 1 & -1 \end{pmatrix} \end{array}$$

The last two rows are zero so we can omit them. The matrix Q consists of the columns corresponding to 2 and 8. Therefore the matrix representing the matroid $\mathcal{M}_S/\mathrm{Rev}$ is

$$D = \begin{array}{c} \begin{array}{ccccc} \boxed{2} & \boxed{8} & \boxed{1} & \boxed{6} & \boxed{7} \end{array} \\ \begin{pmatrix} -1 & 0 & 1 & 0 & 0 \\ 0 & -1 & 0 & 1 & -1 \end{pmatrix} \end{array},$$

which after reordering of the columns is the matrix T in Example 3 of the main text.

For our computational experiments, we used the software toolbox `SAGE` (`http://www.sagemath.org`) for oriented matroids (The Sage Developers, 2016).

4 Computing iMCSs as hitting sets

Given the set of MMBs of a network $\mathcal{N}$, computing the iMCSs of $\mathcal{N}$ is a *hitting set problem*. In general, this has the following form: Given a set of elements Ω and a family Λ of subsets $D \subseteq \Omega$, find (inclusion-)minimal subsets $I \subseteq \Omega$ that contain at least one element in each set of Λ, i.e., $I \cap D \neq \emptyset$, for all $D \in \Lambda$. In our case, $\Omega = \mathrm{Irr}$ and $\Lambda = \mathrm{MMBs}_{tar}$ is the family of MMBs involving the target reaction. We assume that there are no blocked reactions in the network, i.e., reactions which always have zero flux.

We solve the hitting set problem by mixed-integer linear programming. With every subset $I \subseteq \mathrm{Irr}$ we associate a vector $x \in \{0,1\}^{|\mathrm{Irr}|}$ such that $x_j = 1$ if reaction $j \in I$, and $x_j = 0$ if reaction $j \notin I$. The mixed-integer linear program to enumerate iMCSs of minimum cardinality is

$$\begin{aligned} &\text{minimize} \sum_{j\in\mathrm{Irr}} x_j \\ &\text{subject to} \sum_{j\in D} x_j \geq 1,\ \forall D \in \mathrm{MMBs}_{tar}, \\ &\qquad x_j \in \{0,1\}. \end{aligned}$$

Our goal is to enumerate all iMCSs and not only those of minimum cardinality. So whenever we find a new solution x^* at iteration i, we add a linear inequality to reject this solution at iteration $i+1$. If x is a candidate solution at iteration $i+1$, we require $\mathrm{supp}(x^*) \not\subseteq \mathrm{supp}(x)$, which can be formulated as $\sum_{j\in\mathrm{supp}(x^*)} x_j \leq |\mathrm{supp}(x^*)| - 1$.

5 Proofs

Proposition 1. *Let Γ be a flux cone. If $x \geq 0$ for all $x \in \Gamma$, then Γ is pointed and the extreme rays of Γ are exactly the rays in Γ of minimal support.*

Proof. In (Schuster and Hilgetag, 1994; Gagneur and Klamt, 2004), this result is proven for flux cones $\Gamma = \Gamma_{\mathcal{N}}$ originating from a metabolic network $\mathcal{N}$. In this case, Prop. 1 states that in a metabolic network where all reactions are irreversible the extreme rays of $\Gamma_{\mathcal{N}}$ are exactly the EFMs. The proof in (Schuster and Hilgetag, 1994; Gagneur and Klamt, 2004) directly carries over to the more general case of flux cones in the sense of Def. 2 of the main text for which $I = \{1,\ldots,n\}$. □.

Theorem 1. *Let $\Gamma = \{x \in \mathbb{R}^n \mid Ax \geq 0\}$ be a flux cone with $A = \begin{pmatrix} B \\ -B \\ E_{I,*} \end{pmatrix}$. For any $H \supseteq I$ the projection $\mathrm{proj}_H(\Gamma)$ is again a flux cone.*

Proof. For any $k \in \{1,\ldots,n\}$ the projection in direction of k on the set $H_k = \{1,\ldots,n\} \setminus \{k\}$ can be realised by Fourier-Motzkin elimination, see e.g. (Ziegler, 1995). Here a matrix $A^{/k}$ is constructed such that $\mathrm{proj}_{H_k}(\Gamma) = \{x \in \mathbb{R}^n \mid A^{/k}x \geq 0, x_k = 0\}$. The matrix $A^{/k}$ contains the following rows:

- the rows $A_{i,*}$ from A, for all i with $a_{i,k} = 0$.
- the rows $a_{i,k}A_{j,*} + (-a_{j,k})A_{i,*}$, for all i,j with $a_{i,k} > 0, a_{j,k} < 0$.

For the sake of convenience we divide the row indices of A into three sets:

$$J^0 = \{i \mid a_{i,k} = 0\},\quad J^+ = \{i \mid a_{i,k} > 0\},\quad J^- = \{i \mid a_{i,k} < 0\}.$$

If $k \notin I$ then J^0 will contain all rows corresponding to $E_{I,*}$. J^0 can contain rows corresponding to B as well. Furthermore we have $A_{J^+,*} = -A_{J^-,*}$ because A describes a flux cone. Following from this, the rows of $A^{/k}$ can be ordered such that $A^{/k} = \begin{pmatrix} C \\ -C \\ E_{I,*} \end{pmatrix}$ and therefore $\mathrm{proj}_{H_k}(\Gamma)$ is a flux cone as well. Repeating this construction for all $k \notin H \supseteq I$, we conclude that $\mathrm{proj}_H(\Gamma)$ is again a flux cone. □

Theorem 2. *Let $\Gamma_{\mathcal{N}} = \{v \in \mathbb{R}^{|\mathfrak{R}|} \mid Sv = 0,\ v_{\mathrm{Irr}} \geq 0\}$ be the flux cone of a metabolic network $\mathcal{N} = (\mathfrak{M}, \mathfrak{R}, S, \mathrm{Irr})$. The supports of the extreme rays of the pointed cone $\mathrm{proj}_{\mathrm{Irr}}(\Gamma_{\mathcal{N}})$ are exactly the minimal metabolic behaviours of the network $\mathcal{N}$.*

Proof. By Theorem 1 the cone $\mathrm{proj}_{\mathrm{Irr}}(\Gamma_{\mathcal{N}})$ is a flux cone. Furthermore, we have $v \geq 0$, because $v_{\mathrm{Irr}} \geq 0$ and $v_{\mathrm{Rev}} = 0$. Thus $\mathrm{proj}_{\mathrm{Irr}}(\Gamma_{\mathcal{N}})$ is pointed and we may apply Prop. 1 to conclude that the extreme rays of $\mathrm{proj}_{\mathrm{Irr}}(\Gamma_{\mathcal{N}})$ are the rays in $\mathrm{proj}_{\mathrm{Irr}}(\Gamma_{\mathcal{N}})$ with minimal support. Since the supports of the rays in $\mathrm{proj}_{\mathrm{Irr}}(\Gamma_{\mathcal{N}})$ are just the metabolic behaviors in $\mathcal{N}$, the result follows. □.

Theorem 3. *The minimal metabolic behaviors of a metabolic network $\mathcal{N} = (\mathfrak{M}, \mathfrak{R}, S, \mathrm{Irr})$ with flux cone $\Gamma_{\mathcal{N}}$ are exactly the oriented circuits X of the contraction $\mathrm{contr}_{\mathrm{Irr}}(\mathcal{M}_S)$ for which $X^- = \emptyset$. If $T \in \mathbb{R}^{k\times|\mathrm{Irr}|}$ is a matrix representing $\mathrm{contr}_{\mathrm{Irr}}(\mathcal{M}_S)$ then*

$$\mathrm{proj}_{\mathrm{Irr}}(\Gamma_{\mathcal{N}}) = \{v \in \mathbb{R}^{|\mathfrak{R}|} \mid Tv_{\mathrm{Irr}} = 0, v_{\mathrm{Irr}} \geq 0, v_{\mathrm{Rev}} = 0\}.$$

Proof. Let $\mathrm{contr}_{\mathrm{Irr}}(\mathcal{M}_S) = (\mathrm{Irr}, \mathcal{C}_{\mathrm{Irr}})$ be the contraction of $\mathcal{M}_S = (\mathfrak{R}, \mathcal{C})$ to Irr. Let C^{pos}_{Irr} be the family of circuits $X \in \mathcal{C}_{\mathrm{Irr}}$ with $X^- = \emptyset$. Then

$$\begin{aligned} \mathcal{C}^{pos}_{\mathrm{Irr}} &= \mathrm{Min}(\{Y|_{\mathrm{Irr}} \mid Y \in \mathcal{C}\}) \cap \{X \mid X^- = \emptyset\} \\ &= \mathrm{Min}(\{Y|_{\mathrm{Irr}} \mid Y \in \mathcal{C},\ Y^- \cap \mathrm{Irr} = \emptyset\}) \\ &= \mathrm{Min}(\{Y|_{\mathrm{Irr}} \mid \\ &\quad Y \in \mathrm{Min}(\{\sigma(v) \mid Sv = 0, v \in \mathbb{R}^{|\mathfrak{R}|}\}), Y^- \cap \mathrm{Irr} = \emptyset\}) \\ &= \mathrm{Min}(\{Y|_{\mathrm{Irr}} \mid \\ &\quad Y \in \mathrm{Min}(\{\sigma(v) \mid Sv = 0, v_{\mathrm{Irr}} \geq 0, v \in \mathbb{R}^{|\mathfrak{R}|}\})\}) \\ &= \mathrm{Min}(\{\sigma(v)|_{\mathrm{Irr}} \mid Sv = 0, v_{\mathrm{Irr}} \geq 0, v \in \mathbb{R}^{|\mathfrak{R}|}\}) \end{aligned}$$

The last set just defines the MMBs in $\mathcal{N}$.

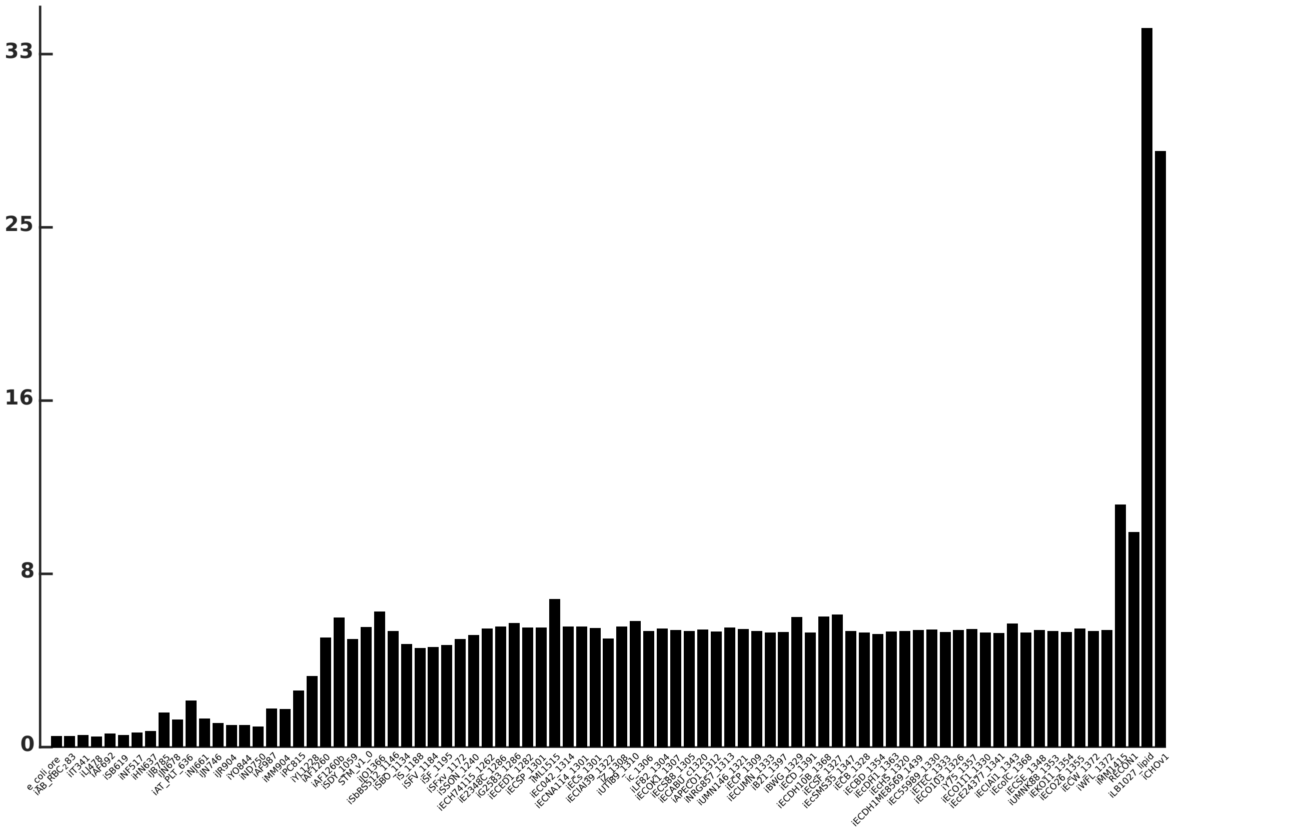

Fig. 1. The 84 networks from the `BiGG Models Database` ordered by the number of reactions. For each network, the bar indicates the time in minutes needed to compute the projected flux cone via contraction. For details, see Tab. 1-2.

If T represents $\mathrm{contr}_{\mathrm{Irr}}(\mathcal{M}_S)$, then $\mathcal{C}_{\mathrm{Irr}} = \mathrm{Min}(\{\sigma(x) \mid Tx = 0, x \in \mathbb{R}^{|\mathrm{Irr}|}\})$. It follows that

$$\begin{aligned}\mathcal{C}_{\mathrm{Irr}}^{pos} &= \mathrm{Min}(\{\sigma(x) \mid Tx = 0, x \geq 0, x \in \mathbb{R}^{|\mathrm{Irr}|}\}) \\ &= \mathrm{Min}(\{\sigma(v)|_{\mathrm{Irr}} \mid Sv = 0, v_{\mathrm{Irr}} \geq 0, v \in \mathbb{R}^{|\mathfrak{R}|}\}) \\ &= \mathrm{Min}(\{\mathrm{supp}(\mathrm{proj}_{\mathrm{Irr}}(v)) \mid v \in \Gamma_{\mathcal{N}}\})\end{aligned}$$

Thus, in $\mathbb{R}^{|\mathfrak{R}|}$, the two pointed cones $\{v \in \mathbb{R}^{|\mathfrak{R}|} \mid Tv_{\mathrm{Irr}} = 0, v_{\mathrm{Irr}} \geq 0, v_{\mathrm{Rev}} = 0\}$ and $\mathrm{proj}_{\mathrm{Irr}}(\Gamma_{\mathcal{N}})$ have the same set of minimal support vectors. By Prop. 1 they have the same set of extreme rays and therefore are identical. □

6 Results

All computations were done on a desktop computer with eight processors Intel(R) Core(TM) i7-2600, CPU 3.40GHZ, each with 2 threads.

6.1 Projection

We used the software `SAGE` (The Sage Developers, 2016) for computing the projection via contraction. We performed the projection on all 84 networks of the `BiGG Models Database` (King *et al.*, 2016), which took between 32 seconds (for a network of 87 unblocked reactions) and 35 minutes (for a network of 4047 unblocked reactions), see Fig. 1 and Tab. 1-2.

6.2 Computing iMCSs using MMBs

For computing the MMBs, we implemented our method in `MATLAB`. We used the software `SAGE` (The Sage Developers, 2016) for computing the projection via contraction and the software `polco` (`http://www.csb.ethz.ch/tools/software/polco.html`) (Terzer, 2009) for enumerating the extreme rays. Given the set of MMBs, computing iMCSs becomes a hitting set problem, see Sect. 4 or (Klamt, 2006).

To evaluate our method, we considered a selection of medium-sized metabolic networks from the `BioModels Database` (Li *et al.*, 2010). The number of *unblocked* reactions, i.e., reactions whose steady-state flux is not always zero, ranges from 87 up to 444. While EFMs could be computed for only one network, the set of MMBs could be obtained for all these networks in a relatively short amount of time, see Tab. 1 in the main document.

The number of MMBs ranges between 82 and 150132 and is not related to the number of irreversible reactions. For example, the network containing 41 irreversible reactions has more MMBs than the network containing 316 irreversible reactions. All networks contain a biomass reaction, which we used as target reaction to compute all iMCSs. The metabolic reconstruction *Rhizobium etli* iOR363 (Resendis-Antonio *et al.*, 2007; Li *et al.*, 2010) contains several biomass reactions, from which we used the *Wildtype Objective Function* with the id `OF14e_Retli`.

The only network for which we were able to compute the whole set of EFMs is *Escherichia coli* MG1655. Here, the number of MMBs is by several orders of magnitude smaller than the number of EFMs, thus computing iMCSs is less time consuming. However, the more sets we have to hit, the more MCSs we obtain. The number of iMCSs is indeed

network id	size original cone	size projected cone	time
e_coli_core	68 × 87	16 × 40	32
iAB_RBC_283	333 × 453	136 × 264	32
iIT341	381 × 436	213 × 276	34
iLJ478	331 × 385	171 × 228	30
iAF692	417 × 484	245 × 321	39
iSB619	381 × 450	192 × 275	35
iNF517	435 × 513	203 × 296	42
iHN637	448 × 524	266 × 351	46
iJB785	671 × 741	440 × 543	100
iJN678	597 × 675	405 × 497	79
iAT_PLT_636	738 × 1008	316 × 559	134
iNJ661	579 × 740	335 × 515	82
iJN746	539 × 652	283 × 401	69
iJR904	450 × 667	243 × 475	63
iYO844	500 × 657	220 × 385	63
iND750	479 × 631	210 × 381	59
iAF987	708 × 840	429 × 574	111
iMM904	650 × 893	307 × 586	109
iPC815	761 × 1065	450 × 774	163
iYL1228	830 × 1223	495 × 925	205
iAF1260	1032 × 1532	661 × 1185	316
iAF1260b	1040 × 1554	662 × 1200	373
iSDY_1059	1026 × 1502	627 × 1133	311
STM_v1_0	1086 × 1597	711 × 1249	346
iJO1366	1155 × 1705	732 × 1312	391
iSbBS512_1146	1018 × 1540	622 × 1169	334
iSBO_1134	1022 × 1530	630 × 1168	297
iS_1188	1017 × 1504	604 × 1127	286
iSFV_1184	1026 × 1516	605 × 1136	288
iSF_1195	1022 × 1512	601 × 1129	294
iSF×v_1172	1045 × 1554	627 × 1171	311
iSSON_1240	1066 × 1601	638 × 1206	323
iECH74115_1262	1083 × 1636	658 × 1246	342
iE2348C_1286	1087 × 1641	657 × 1243	347
iG2583_1286	1087 × 1644	662 × 1254	358
iECED1_1282	1087 × 1644	657 × 1249	344
iECSP_1301	1087 × 1646	662 × 1256	344
iML1515	1147 × 1744	719 × 1350	427
iEC042_1314	1084 × 1644	662 × 1257	347
iECNA114_1301	1091 × 1656	660 × 1260	348
iECs_1301	1087 × 1646	662 × 1256	343

Table 1. Sizes of the flux cones and time for the projection for the first 42 networks (w.r.t. the number of reactions) of the `BiGG Models Database` (King et al., 2016). **network id**: The id of the network in the `BiGG Models Database`. **size original cone**: size of the flux cone of the original network: unblocked reactions and non-dead end metabolites. **size projected cone**: size of the projected flux cone of the original network: number of columns and rows of the matrix describing the projected flux cone. **time**: time in seconds needed to project onto the irreversible reactions (using the network without the blocked reactions).

network id	size original cone	size projected cone	time
iECIAI39_1322	1044 × 1569	613 × 1177	313
iZ_1308	1087 × 1646	662 × 1256	347
iUTI89_1310	1096 × 1662	660 × 1261	363
ic_1306	1090 × 1656	654 × 1254	334
iLF82_1304	1082 × 1650	645 × 1243	342
iECOK1_1307	1096 × 1670	660 × 1269	337
iECS88_1305	1088 × 1653	660 × 1260	335
iECABU_c1320	1094 × 1663	659 × 1262	339
iAPECO1_1312	1096 × 1668	660 × 1267	333
iNRG857_1313	1100 × 1675	660 × 1268	344
iUMN146_1321	1096 × 1670	660 × 1269	341
iECP_1309	1094 × 1668	659 × 1267	334
iECUMN_1333	1093 × 1657	655 × 1255	330
iB21_1397	1089 × 1650	658 × 1253	332
iBWG_1329	1164 × 1739	726 × 1335	375
iECD_1391	1089 × 1650	658 × 1253	330
iECDH10B_1368	1160 × 1736	721 × 1331	376
iECSF_1327	1162 × 1743	726 × 1338	382
iEcSMS35_1347	1102 × 1673	664 × 1271	334
iECB_1328	1096 × 1660	662 × 1262	331
iECBD_1354	1089 × 1651	658 × 1254	326
iEcDH1_1363	1099 × 1667	663 × 1266	333
iEcHS_1320	1094 × 1645	662 × 1251	334
iECDH1ME8569_1439	1101 × 1670	663 × 1268	338
iEC55989_1330	1103 × 1670	664 × 1268	339
iETEC_1333	1095 × 1658	664 × 1263	332
iECO103_1326	1096 × 1660	661 × 1262	338
iY75_1357	1101 × 1670	663 × 1268	340
iECO111_1330	1089 × 1651	660 × 1259	330
iEcE24377_1341	1092 × 1655	663 × 1260	329
iECIAI1_1343	1089 × 1638	663 × 1251	356
iEcolC_1368	1092 × 1653	663 × 1261	331
iECSE_1348	1098 × 1664	663 × 1266	337
iUMNK88_1353	1098 × 1665	664 × 1268	334
iEKO11_1354	1098 × 1655	663 × 1257	332
iECO26_1355	1098 × 1666	663 × 1268	342
iECW_1372	1102 × 1668	665 × 1269	334
iWFL_1372	1102 × 1668	665 × 1269	337
iMM1415	1665 × 2432	855 × 1576	700
RECON1	1586 × 2467	525 × 1314	620
iLB1027_lipid	1814 × 4047	1355 × 3653	2075
iCHOv1	2213 × 4280	943 × 2527	1720

Table 2. Sizes of the flux cones and time for the projection for the second 42 networks (w.r.t. the number of reactions) in the `BiGG Models Database` (King et al., 2016). **network id**: The id of the network on the `BiGG Models Database`. **size original cone**: size of the flux cone of the original network: unblocked reactions and non-dead end metabolites. **size projected cone**: size of the projected flux cone of the original network: number of columns and rows of the matrix describing the projected flux cone. **time**: time in seconds needed to project onto the irreversible reactions (using the network without the blocked reactions).

smaller than the number of MCSs, and we are able to compute all of them in a short amount of time, see Tab. 1 in the main document. The time to compute iMCSs includes checking the results. For each iMCSs ζ we ensure that removing all the reactions in ζ from the network implies a zero flux through the target reaction. This checking step accounts for most of the running time.

The cardinalities of the iMCS we found are given in Fig. 2 and Tab. 3. Note that working with MMBs allows us to determine *all iMCSs* for the target reaction in the corresponding network.

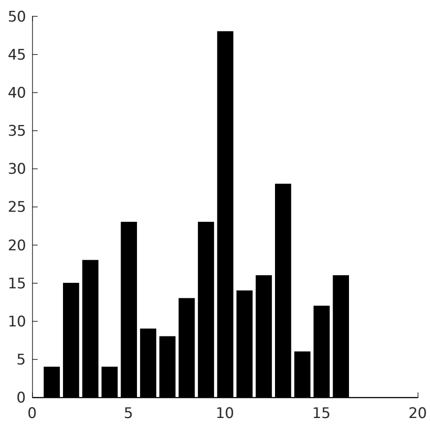

Fig. 2. Cardinality of iMCSs for *Escherichia coli* MG1655 (King et al., 2016). Each bar illustrates the number of iMCSs of the cardinality given on the x-axis. The number of iMCSs can be found on the y-axis.

network	rxns	irr	iMCSs	cardinality															
				1	2	3	4	5	6	7	8	9	10	11	12	13	14	15	16
Escherichia coli MG1655 (Orth *et al.*, 2010)	87	41	257	4	15	17	4	23	9	8	13	23	48	13	16	29	6	13	16
Rhizobium etli iOR363 (Resendis-Antonio *et al.*, 2007)	194	104	60	29	18	13	0	0	0	0	0	0	0	0	0	0	0	0	0
Buchnera iSM197 (MacDonald *et al.*, 2011)	244	170	200	165	18	11	6	0	0	0	0	0	0	0	0	0	0	0	0
Blattabacterium cuenoti iCG238 (González-Domenech *et al.*, 2012)	308	197	184	165	6	9	4	0	0	0	0	0	0	0	0	0	0	0	0
Blattabacterium iCG230 (González-Domenech *et al.*, 2012)	400	192	159	152	7	0	0	0	0	0	0	0	0	0	0	0	0	0	0
Mycobacterium tuberculosis iNJ661 (Jamshidi and Palsson, 2007)	427	296	381	233	102	20	26	0	0	0	0	0	0	0	0	0	0	0	0
Salmonella Typhimurium STM_v1_0 (Thiele *et al.*, 2011)	458	316	321	296	19	6	0	0	0	0	0	0	0	0	0	0	0	0	0
Helicobacter pylori iCS291 (Schilling *et al.*, 2002)	444	271	187	95	37	14	19	2	7	13	0	0	0	0	0	0	0	0	0

Table 3. Cardinality of iMCSs for selected networks (with given target reaction). The description of *Escherichia coli* MG1655 (Orth et al., 2010) was taken from the `BiGG Models Database` (King et al., 2016), while the remaining ones come from the `BioModels Database` (Li et al., 2010). **network**: name of the metabolic network. **rxns**: number of unblocked reactions. **irr**: number of unblocked irreversible reactions. **iMCS**: number of irreversible minimal cut sets. **cardinality**: number of all existing iMCSs of the corresponding cardinality.

6.3 Computing iMCSs using the dual approach

6.3.1 Computing iMCSs with `CellNetAnalyzer`

In the following, we present results for computing a given number of iMCSs using the toolbox `CellNetAnalyzer` (von Kamp *et al.*, 2017), version 2018.1, together with `CPLEX 12.8` (`http://www.cplex.com`). We computed iMCSs using the original and the projected flux cone for all networks from the `BiGG Models Database` (King *et al.*, 2016) that include a biomass reaction (which was the target reaction). When searching for MCSs in the original flux cone, we only allowed irreversible reactions to be included in the computed MCSs. Thus, we computed iMCSs also in the original flux cone.

The results are summarised graphically in Fig. 4 of the main document. Tab. 4 to 7 provide the full information. In each experiment, we specify a number of iMCSs to be computed. In general, `CellNetAnalyzer` computes slightly more than the requested number due to internal algorithmic reasons. An entry 'OoM' indicates that `CellNetAnalyzer` ran out of memory. Note that for various larger genome-scale metabolic networks, it was not possible to compute any iMCSs using the original cone, while in all these cases we were able to compute 40 or more iMCSs using the projected cone. For all networks considered here with the exception of `e_coli_core`, we were only able to compute iMCSs of cardinality 1.

network id	pre-nr	nr original	nr projected	time original	time projected	relative time
e_coli_core	10	15	18	1	0.41	2.44
	20	33	33	2.72	0.84	3.24
	50	57	55	1.21	0.61	1.98
	100	110	111	2.17	5	0.43
iIT341	10	15	10	5.49	2.33	2.36
	20	24	40	6.39	2.51	2.55
	50	58	54	5.32	2.42	2.20
iLJ478	10	10	11	4.4	1.88	2.34
	20	21	20	3.96	1.87	2.12
	50	51	50	4.12	1.81	2.28
iAF692	10	11	11	5.69	2.73	2.08
	20	22	20	6.01	2.73	2.20
	50	51	58	6	2.98	2.01
iSB619	10	10	12	5.06	2.24	2.26
	20	21	23	4.94	2.23	2.22
	50	51	62	5.25	2.38	2.21
iNF517	10	10	11	5.82	2.48	2.35
	20	20	22	5.78	2.44	2.37
	50	51	58	6.17	2.65	2.33
iHN637	10	12	12	6.24	3.05	2.05
	20	22	22	6.24	3.03	2.06
	50	58	57	6.51	3.27	1.99
iJB785	50	50	59	18.34	7.38	2.49
iJN678	10	11	26	9.5	6.46	1.47
	20	23	29	14.8	5.96	2.48
	50	54	67	12.19	5.85	2.08
iNJ661	10	12	11	16.44	6.25	2.63
	20	20	21	13.35	6.11	2.18
	50	50	50	14.19	6.73	2.11
	100	101	101	16.49	7.17	2.30
iJN746	10	13	12	9.33	3.77	2.47
	20	21	21	9.69	3.83	2.53
	50	51	50	9.78	4.14	2.36
	100	102	100	10.33	4.12	2.51
iJR904	10	10	10	10.23	5.66	1.81
	20	20	20	10.77	5.92	1.82
	50	65	51	11.5	6.35	1.81
	100	124	108	10.85	6.59	1.65

Table 4. **network id**: id of the network in the `BiGG Models Database`. **pre-nr**: requested number of iMCSs. **nr original**: number of iMCSs computed using the original cone, in general at least as many as requested. **nr projected**: number of iMCSs computed using the projected cone, in general at least as many as requested. **time original**: time (in seconds) needed to compute the given number of iMCSs in the original cone. **time projected**: time (in seconds) needed to compute the given number of iMCSs in the projected cone. **relative time**: relative time needed to compute the given number of iMCSs in the original cone compared to the time needed using the projected cone.

network id	pre-nr	nr original	nr projected	time original	time projected	relative time
iYO844	10	12	11	9.5	3.56	2.67
	20	20	20	10.09	3.78	2.67
	50	53	50	10.68	4.05	2.64
	100	106	100	10.34	4.19	2.47
iND750	10	13	10	9.11	3.57	2.55
	20	25	21	9.12	3.7	2.46
	50	53	50	9.97	3.9	2.56
	100	106	100	9.67	3.72	2.60
iAF987	10	10	10	15.96	6.89	2.32
	20	23	25	16.93	7.23	2.34
	50	60	68	20.58	7.31	2.82
	100	110	119	16.89	7.14	2.37
iMM904	10	12	10	19.44	7.7	2.52
	20	22	20	20.16	8.23	2.45
	50	51	50	26.59	8.91	2.98
	100	101	102	19.84	10.85	1.83
iPC815	10	11	10	28.61	13.22	2.16
	20	20	20	30.13	13.94	2.16
	100	100	101	29.24	14.08	2.08
iYL1228	10	10	10	40.66	20.24	2.01
	20	20	20	42.29	20.95	2.02
	100	102	100	42.47	20.54	2.07
iAF1260	10	10	10	67.14	37.18	1.81
	20	20	20	76.99	40.11	1.92
	100	101	101	68.32	42.66	1.60
iAF1260b	10	10	10	69.72	37.52	1.86
	20	20	20	80.36	41.85	1.92
	40	40	40	93.02	53.18	1.75
	100	101	102	71	55.26	1.28
iSDY_1059	10	10	10	65.95	31.78	2.08
	20	20	27	70.23	34.95	2.01
	40	40	41	75.56	37.68	2.01
	100	100	122	67.22	37.74	1.78
STM_v1_0	10	10	11	77.27	41.58	1.86
	20	20	20	83.27	44.78	1.86
	40	40	41	89.25	50.11	1.78
	100	101	100	78.29	49.96	1.57
iJO1366	10	10	10	94.75	46.35	2.04
	20	21	23	100.32	50.66	1.98
	40	43	50	113.93	56.41	2.02
	100	111	107	117.53	56.1	2.10
iSbBS512_1146	10	11	11	67.98	34.65	1.96
	20	20	23	73.41	37.34	1.97
	40	44	50	80.56	41.55	1.94
	100	135	121	77.1	40.84	1.89
iSBO_1134	10	13	10	69.24	34.38	2.01
	20	22	26	76.12	37.71	2.02
	40	48	49	77.71	41.09	1.89
	100	132	119	78.95	41.11	1.92
iS_1188	10	12	12	65.28	31.63	2.06
	20	20	26	70.15	34.48	2.03
	40	40	53	75.28	38.45	1.96
	100	124	109	79.25	37.66	2.10
iSFV_1184	10	11	12	67.54	32.62	2.07
	20	20	26	73.33	35.72	2.05
	40	40	52	75.5	38.4	1.97
	100	133	116	74.25	38.82	1.91

Table 5. **network id**: id of the network in the `BiGG Models Database`. **pre-nr**: requested number of iMCSs. **nr original**: number of iMCSs computed using the original cone, in general at least as many as requested. **nr projected**: number of iMCSs computed using the projected cone, in general at least as many as requested. **time original**: time (in seconds) needed to compute the given number of iMCSs in the original cone. **time projected**: time (in seconds) needed to compute the given number of iMCSs in the projected cone. **relative time**: relative time needed to compute the given number of iMCSs in the original cone compared to the time needed using the projected cone.

network id	pre-nr	nr original	nr projected	time original	time projected	relative time
iSF_1195	10	14	11	67.07	31.88	2.10
	20	25	23	74.14	34.62	2.14
	40	49	49	74.91	39.09	1.92
	100	114	110	72.69	37.71	1.93
iSFxv_1172	10	10	11	72.9	35.04	2.08
	20	20	26	83.11	38.48	2.16
	40	40	53	85.95	41.18	2.09
	100	100	117	86.48	41.7	2.07
iSSON_1240	10	11	12	35.16	37.92	0.93
	40	41	48	88.32	44.9	1.97
	100	100	131	87.88	44.96	1.95
iECH74115_1262	10	12	13	37.92	40.75	0.93
	40	40	46	94.19	49.24	1.91
	100	117	124	93.73	49.09	1.91
iE2348C_1286	10	13	15	40.75	42.37	0.96
	40	44	42	96.23	48.67	1.98
	100	119	107	95.93	50	1.92
iG2583_1286	10	15	11	42.37	44.86	0.94
	40	47	48	96.97	49.66	1.95
	100	115	112	93.78	50.25	1.87
iECED1_1282	10	14	13	106.35	47.94	2.22
	40	44	47	96.1	49.48	1.94
	100	111	121	93.55	49.71	1.88
iECSP_1301	10	10	15	90.99	46.51	1.96
	40	**OoM**	**49**	**OoM**	**50.35**	**NAN**
iML1515	10	10	11	123.43	57.22	2.16
	40	**OoM**	**40**	**OoM**	**62.58**	**NAN**
iEC042_1314	10	13	14	92.84	46.44	2.00
	40	**OoM**	**53**	**OoM**	**49.77**	**NAN**
iECNA114_1301	10	10	14	107.49	46.62	2.31
	40	**OoM**	**58**	**OoM**	**53.38**	**NAN**
iECs_1301	10	10	11	98.75	45.64	2.16
	40	**OoM**	**50**	**OoM**	**49.77**	**NAN**
iECIAI39_1322	10	10	10	80.24	38.11	2.11
	40	**OoM**	**40**	**OoM**	**41.16**	**NAN**
iZ_1308	10	11	11	91.73	45.8	2.00
	40	**OoM**	**50**	**OoM**	**51.05**	**NAN**
iUTI89_1310	10	10	11	95.72	46.7	2.05
	40	**OoM**	**51**	**OoM**	**50.95**	**NAN**
ic_1306	10	17	12	94.22	45.91	2.05
	40	**OoM**	**57**	**OoM**	**50.32**	**NAN**
iLF82_1304	10	12	12	91.54	44.84	2.04
	40	**OoM**	**46**	**OoM**	**48.61**	**NAN**
iECOK1_1307	10	12	12	104.78	47.24	2.21
	40	**OoM**	**54**	**OoM**	**52.17**	**NAN**
iECS88_1305	10	10	11	97.17	46.42	2.1
	40	**OoM**	**43**	**OoM**	**50.67**	**NAN**
iECABU_c1320	10	12	15	95.62	47.45	2
	40	**OoM**	**48**	**OoM**	**51.2**	**NAN**
iAPECO1_1312	10	10	13	105.84	48.67	2.17
	40	**OoM**	**50**	**OoM**	**51.73**	**NAN**
iNRG857_1313	10	11	10	95.62	49.63	1.92
	40	**OoM**	**49**	**OoM**	**52.09**	**NAN**
iUMN146_1321	10	10	12	95.71	48.03	1.99
	40	**OoM**	**48**	**OoM**	**51.76**	**NAN**

Table 6. **network id**: id of the network in the `BiGG Models Database`. **pre-nr**: requested number of iMCSs. **nr original**: number of iMCSs computed using the original cone, in general at least as many as requested. **nr projected**: number of iMCSs computed using the projected cone, in general at least as many as requested. **time original**: time (in seconds) needed to compute the given number of iMCSs in the original cone. **time projected**: time (in seconds) needed to compute the given number of iMCSs in the projected cone. **relative time**: relative time needed to compute the given number of iMCSs in the original cone compared to the time needed using the projected cone. **OoM**: the program ran out of memory when trying to compute the requested number of iMCSs.

network id	pre-nr	nr original	nr proj	time original	time proj	relative time
iECP_1309	10	10	12	96.49	44.98	2.14
	40	**OoM**	**42**	**OoM**	**51.56**	**NAN**
iECUMN_1333	10	11	13	93.48	46.15	2.02
	40	**OoM**	**59**	**OoM**	**50.72**	**NAN**
iB21_1397	10	15	11	89.75	45.78	1.96
	40	**OoM**	**56**	**OoM**	**50.41**	**NAN**
iBWG_1329	10	15	14	107.72	54.65	1.97
	40	**OoM**	**50**	**OoM**	**59.04**	**NAN**
iECD_1391	10	12	11	91.91	45.42	2.02
	40	**OoM**	**56**	**OoM**	**50.21**	**NAN**
iECDH10B_1368	**10**	**OoM**	**10**	**OoM**	**52.37**	**NAN**
	40	**OoM**	**40**	**OoM**	**57.45**	**NAN**
iECSF_1327	**10**	**OoM**	**10**	**OoM**	**54.19**	**NAN**
	40	**OoM**	**50**	**OoM**	**60.3**	**NAN**
iEcSMS35_1347	**10**	**OoM**	**14**	**OoM**	**47.29**	**NAN**
	40	**OoM**	**45**	**OoM**	**52.41**	**NAN**
iECB_1328	**10**	**OoM**	**12**	**OoM**	**45.67**	**NAN**
	40	**OoM**	**46**	**OoM**	**51.34**	**NAN**
iECBD_1354	**10**	**OoM**	**18**	**OoM**	**45.8**	**NAN**
	40	**OoM**	**43**	**OoM**	**50.61**	**NAN**
iEcDH1_1363	**10**	**OoM**	**13**	**OoM**	**46.45**	**NAN**
	40	**OoM**	**42**	**OoM**	**50.85**	**NAN**
iEcHS_1320	**10**	**OoM**	**10**	**OoM**	**45.07**	**NAN**
	40	**OoM**	**47**	**OoM**	**49.7**	**NAN**
iECDH1ME8569_1439	**10**	**OoM**	**10**	**OoM**	**46.58**	**NAN**
	40	**OoM**	**62**	**OoM**	**51.66**	**NAN**
iEC55989_1330	**10**	**OoM**	**11**	**OoM**	**46.46**	**NAN**
	40	**OoM**	**49**	**OoM**	**51.13**	**NAN**
iETEC_1333	**10**	**OoM**	**11**	**OoM**	**46.44**	**NAN**
	40	**OoM**	**51**	**OoM**	**51.12**	**NAN**
iECO103_1326	**10**	**OoM**	**11**	**OoM**	**46.74**	**NAN**
	40	**OoM**	**47**	**OoM**	**51.71**	**NAN**
iY75_1357	**10**	**OoM**	**10**	**OoM**	**46.52**	**NAN**
	40	**OoM**	**41**	**OoM**	**51.36**	**NAN**
iECO111_1330	**10**	**OoM**	**10**	**OoM**	**45.79**	**NAN**
	40	**OoM**	**41**	**OoM**	**49.8**	**NAN**
iEcE24377_1341	**10**	**OoM**	**12**	**OoM**	**48.58**	**NAN**
	40	**OoM**	**50**	**OoM**	**51.26**	**NAN**
iECIAI1_1343	**10**	**OoM**	**12**	**OoM**	**43.6**	**NAN**
	40	**OoM**	**45**	**OoM**	**49.03**	**NAN**
iEcolC_1368	**10**	**OoM**	**14**	**OoM**	**46.61**	**NAN**
	40	**OoM**	**52**	**OoM**	**52.28**	**NAN**
iECSE_1348	**10**	**OoM**	**10**	**OoM**	**47.44**	**NAN**
	40	**OoM**	**44**	**OoM**	**51.96**	**NAN**
iUMNK88_1353	**10**	**OoM**	**10**	**OoM**	**47.77**	**NAN**
	40	**OoM**	**57**	**OoM**	**52.19**	**NAN**
iEKO11_1354	**10**	**OoM**	**10**	**OoM**	**46.1**	**NAN**
	40	**OoM**	**51**	**OoM**	**53.27**	**NAN**
iECO26_1355	**10**	**OoM**	**10**	**OoM**	**46.9**	**NAN**
	40	**OoM**	**48**	**OoM**	**53.48**	**NAN**
iECW_1372	**10**	**OoM**	**12**	**OoM**	**47.4**	**NAN**
	40	**OoM**	**47**	**OoM**	**53.49**	**NAN**
iWFL_1372	**10**	**OoM**	**12**	**OoM**	**47.38**	**NAN**
	40	**OoM**	**47**	**OoM**	**53.69**	**NAN**
iWFL_1372	**10**	**OoM**	**10**	**OoM**	**84.81**	**NAN**

Table 7. **network id**: id of the network in the `BiGG Models Database`. **pre-nr**: requested number of iMCSs. **nr original**: number of iMCSs computed using the original cone, in general at least as many as requested. **nr proj**: number of iMCSs computed using the projected cone, in general at least as many as requested. **time original**: time (in seconds) needed to compute the given number of iMCSs in the original cone. **time proj**: time (in seconds) needed to compute the given number of iMCSs in the projected cone. **OoM**: the program ran out of memory trying to compute the requested number of iMCSs.

6.3.2 Computing iMCSs including a knock-out reaction

We applied the software of (Tobalina *et al.*, 2016) together with `CPLEX 12.4` (`http://www.cplex.com`) to the original stoichiometric matrices and to the matrices after the projection was performed. Then we compared the results. Again the networks originate from the `BiGG Models Database` (King *et al.*, 2016). Following (Tobalina *et al.*, 2016), we used as target reaction the biomass reaction and looped over all irreversible reactions. For each irreversible reaction i we set a time limit of 1 minute and tried to compute an iMCS using the biomass reaction as a target reaction and i as a knock-out reaction. The computation for i stopped if such an iMCS was found or after the timeout of 1 minute. Finally, we compared the number of iMCSs computed using this approach. Except for one network, we always computed more iMCSs in the projected flux cone than in the original cone, see Tab. 8, and Fig. 5 in the main article.

network id	Nr. original	Nr. projected	difference
iG2583_1286	847	1133	286
iECED1_1282	845	994	149
iECSP_1301	868	996	128
iML1515	877	1350	473
iECNA114_1301	862	1135	273
iECs_1301	866	1007	141
iZ_1308	841	1008	167
iUTI89_1310	841	1032	191
ic_1306	896	1055	159
iLF82_1304	836	1088	252
iECOK1_1307	861	1106	245
iECS88_1305	835	1055	220
iECABU_c1320	855	1090	235
iAPECO1_1312	845	1121	276
iUMN146_1321	831	1037	206
iBWG_1329	937	1226	289
iECD_1391	833	1135	302
iECDH10B_1368	924	1231	307
iECSF_1327	959	1277	318
iEcSMS35_1347	851	1066	215
iECB_1328	871	1183	312
iECBD_1354	824	1078	254
iEcDH1_1363	819	1148	329
iEcHS_1320	854	1150	296
iECDH1ME8569_1439	836	1065	229
iEC55989_1330	858	1080	222
iETEC_1333	844	1061	217
iECO103_1326	846	1108	262
iY75_1357	826	1074	248
iECO111_1330	879	1042	163
iEcE24377_1341	863	1101	238
iECIAI1_1343	854	666	-188
iEcolC_1368	832	1117	285
iECSE_1348	865	1018	153
iUMNK88_1353	830	1023	193
iEKO11_1354	835	1162	327
iECO26_1355	842	1129	287
iWFL_1372	840	1179	339
iLB1027_lipid	546	2916	2370

Table 8. We applied the program of (Tobalina et al., 2016) to the original stoichiometric matrices and to the matrices after the projection was performed. As a target reaction we had for all cases the biomass reaction. We looped over all irreversible reactions and compute an iMCS. After one minute, or after an iMCS was found, the next step started with a new knock-out reaction. **network id:** the id of the network as it can be found in the `BiGG Models Database`. **Nr. original:** the number of iMCSs which were found using the original flux cone. **Nr. projected:** the number of iMCSs which were found using the projected flux cone. **difference:** the number of iMCSs we found more when using the projected flux cone instead the original.

7 Impact of the ratio between reversible and irreversible reactions on the performance of the projection

To study the impact of the ratio between reversible and irreversible reactions on the projection, we did the following additional experiments using the `ecoli_core` network. We first performed the projection on the irreversible reactions using the original network. Then we set the first reversible reaction to irreversible (which also makes some other reactions irreversible) and performed the projection on the new network N_1. In the following step, we set the first reversible reaction of the network N_1 to irreversible and performed the projection. We repeated this procedure until no reaction in the network was reversible anymore. We compared the sizes of the projected flux cones and the computation time. The results are given in Tab. 9. Contrary to what might be expected, the time for the projection seems to increase with the number of irreversible reactions (except for the trivial case where all reactions are irreversible). We believe that in general it is not clear what impact the ratio of irreversible to reversible reactions will have on the computation time for the projection.

network name	size normal	size projected	time
e_coli_core_projected	68×87	16×40	32
ecoli_core_Irrev_step_1_projected	68×87	49×73	32
ecoli_core_Irrev_step_2_projected	68×87	53×77	34
ecoli_core_Irrev_step_3_projected	68×87	55×79	30
ecoli_core_Irrev_step_4_projected	68×87	57×81	39
ecoli_core_Irrev_step_5_projected	68×87	58×82	35
ecoli_core_Irrev_step_6_projected	68×87	59×83	42
ecoli_core_Irrev_step_7_projected	68×87	62×86	46
ecoli_core_Irrev_step_8_projected	68×87	63×87	53
ecoli_core_Irrev_step_9_projected	68×87	68×87	0

Table 9. Given the `e_coli_core` network, we set step-by-step one reversible reaction to irreversible and perform the projection on the new set of irreversible reactions. Each row corresponds to one step: in the first row the projection was applied to the original flux cone. In the second row, the projection was performed on the network after setting one reversible reaction to irreversible, etc. **network name**: the name of the network and the step resp. number of reversible reactions set to irreversible. **size normal** is the size of the original flux cone (number of metabolites times the number of reactions). **size projected** gives the size of the cone after the projection was performed and **time** gives the time in seconds, needed to perform the projection.

References

Björner, A., Las Vergnas, M., Sturmfels, B., White, N., and Ziegler, G. M. (1999). *Oriented matroids*, volume 2. Cambridge University Press.

Gagneur, J. and Klamt, S. (2004). Computation of elementary modes: a unifying framework and the new binary approach. *BMC Bioinformatics*, **5**(175).

González-Domenech, C. M., Belda, E., Patiño-Navarrete, R., Moya, A., Peretó, J., and Latorre, A. (2012). Metabolic stasis in an ancient symbiosis: genome-scale metabolic networks from two *Blattabacterium cuenoti* strains, primary endosymbionts of cockroaches. *BMC Microbiology*, **12**(Suppl 1), S5.

Jamshidi, N. and Palsson, B. Ø. (2007). Investigating the metabolic capabilities of *Mycobacterium tuberculosis* H37Rv using the *in silico strain iNJ*661 and proposing alternative drug targets. *BMC Systems Biology*, **1**(26).

King, Z. A., Lu, J., Dräger, A., Miller, P., Federowicz, S., Lerman, J. A., Ebrahim, A., Palsson, B. Ø., and Lewis, N. E. (2016). BiGG Models: A platform for integrating, standardizing and sharing genome-scale models. *Nucleic Acids Research*, **44**(D1), D515–D522.

Klamt, S. (2006). Generalized concept of minimal cut sets in biochemical networks. *Biosystems*, **83**(2–3), 233–247.

Li, C., Donizelli, M., Rodriguez, N., Dharuri, H., Endler, L., Chelliah, V., Li, L., He, E., Henry, A., Stefan, M. I., *et al.* (2010). BioModels Database: An enhanced, curated and annotated resource for published quantitative kinetic models. *BMC Systems Biology*, **4**(92).

MacDonald, S. J., Thomas, G. H., and Douglas, A. E. (2011). Genetic and metabolic determinants of nutritional phenotype in an insect–bacterial symbiosis. *Molecular Ecology*, **20**(10), 2073–2084.

Orth, J. D., Fleming, R. M., and Palsson, B. Ø. (2010). Reconstruction and Use of Microbial Metabolic Networks: the Core *Escherichia coli* Metabolic Model as an Educational Guide. *EcoSal plus*.

Resendis-Antonio, O., Reed, J. L., Encarnación, S., Collado-Vides, J., and Palsson, B. Ø. (2007). Metabolic Reconstruction and Modeling of Nitrogen Fixation in *Rhizobium etli*. *PLoS Computational Biology*, **3**(10), e192.

Schilling, C. H., Covert, M. W., Famili, I., Church, G. M., Edwards, J. S., and Palsson, B. Ø. (2002). Genome-Scale Metabolic Model of *Helicobacter pylori* 26695. *Journal of Bacteriology*, **184**(16), 4582–4593.

Schuster, S. and Hilgetag, C. (1994). On elementary flux modes in biochemical reaction systems at steady state. *Journal of Biological Systems*, **2**(02), 165–182.

Terzer, M. (2009). *Large scale methods to enumerate extreme rays and elementary modes*. Ph.D. thesis, ETH Zurich.

The Sage Developers (2016). *SageMath, the Sage Mathematics Software System (Version 7.4.1)*. http://www.sagemath.org.

Thiele, I., Hyduke, D. R., Steeb, B., Fankam, G., Allen, D. K., Bazzani, S., Charusanti, P., Chen, F.-C., Fleming, R. M. T., Hsiung, C. A., *et al.* (2011). A community effort towards a knowledge-base and mathematical model of the human pathogen *Salmonella* Typhimurium LT2. *BMC Systems Biology*, **5**, 8.

Tobalina, L., Pey, J., and Planes, F. J. (2016). Direct calculation of minimal cut sets involving a specific reaction knock-out. *Bioinformatics*, **32**(13), 2001–2007.

von Kamp, A., Thiele, S., Hädicke, O., and Klamt, S. (2017). Use of *CellNetAnalyzer* in biotechnology and metabolic engineering. *J Biotechnol.*, **261**, 221–228.

Ziegler, G. M. (1995). *Lectures on Polytopes*, volume 152. Springer Science & Business Media.